Proceedings of the Indian National Science Academy (2026) 92:1316–1328
https://doi.org/10.1007/s43538-025-00528-6

RESEARCH PAPER

# Influence of recycled coarse aggregate for grouting on the mechanical properties and frost resistance of concrete

**Mengting Fan**[1] · **Xuan Wang**[2]

Received: 9 October 2024 / Accepted: 18 August 2025 / Published online: 8 September 2025
© Indian National Science Academy 2025

**Abstract**
As a product of recycling and reusing construction waste, recycled coarse aggregate not only effectively alleviates the shortage of natural aggregate resources, but also reduces the environmental pollution caused by construction waste. To systematically analyze the influence of slurry containing recycled aggregates on the mechanical properties and frost resistance of recycled concrete, a study was conducted on the slurry treatment of recycled coarse aggregate using ordinary Portland cement, silica powder, and sulfoaluminate cement, and the mixing ratio of concrete was constructed. Meanwhile, the calculation methods for the mechanical and frost resistance indicators of concrete are explained. The results showed that the average maximum values of compressive strength within the recycled concrete group at 3 d, 7 d, and 28 d were 41.87 MPa, 48.73 MPa, and 55.15 MPa, respectively. As the number of freeze–thaw cycles increased, the relative dynamic modulus of the test block gradually decreased. In summary, grouting treatment can optimize the mechanical and freeze–thaw resistance properties of recycled concrete. This research result can provide technical support for the reuse of construction waste.

**Keywords** Patina · Recycled coarse aggregate · Concrete · Dynamics · Frost resistance · Performance

## Introduction

The advancement of urbanization has promoted the development of urban construction, while large-scale urban construction has also generated a large amount of construction waste. Waste concrete accounts for a significant portion of construction waste (Gharibi and Mostofinejad 2023). The commonly used methods for the treatment of construction waste include roadbed and foundation cushion, stacking, and landfilling. However, these methods still cause damage to the natural environment and waste resources (Chen et al. 2022; Supsup et al. 2023). Therefore, it is necessary to find suitable methods to recycle the waste concrete in construction waste. Recycled concrete is one of the ways to solve this problem. After the waste concrete blocks are crushed, different particle sizes of recycled aggregates can be obtained through screening, which can then be used to replace natural aggregates and prepare recycled concrete (Li et al. 2024). However, the effect of pure recycled concrete is even worse than that of simple concrete. To solve the problem of recycled concrete, commonly used methods include modification treatment, such as physical methods, introduction of self compacting concrete, chemical methods, introduction of fiber materials, hydration cement slurry modification, etc. (Yousheng et al. 2023).

He et al. designed a modification method using volcanic ash slurry combined with water glass and silicon-based additives to treat coarse aggregates for recycled bricks, and analyzed the microstructure of recycled concrete using mercury intrusion porosimetry and scanning electron microscopy. The physical properties of the processed aggregate have been improved, and the Compressive Strength (CS) and resistance to chloride ion penetration have also been significantly enhanced (He et al. 2024). Li et al. conducted a composite impregnation treatment on recycled concrete using sodium silicate solution and silane slurry to understand the performance of recycled concrete as a function of substitution rate. They replaced natural aggregates with

✉ Xuan Wang
15923932029@163.com

[1] School of Architectural Engineering, Chongqing City Vocational College, Chongqing 402160, China

[2] College of Urban Construction Engineering, Chongqing University of Arts and Sciences, Chongqing 402160, China

different proportions of substitution rates and mixed Recycled Coarse Aggregates (RCA) into general concrete. The Water Absorption Rate (WAR) of modified recycled concrete decreased the most significantly, reaching 52.8% (Li et al. 2023a). Liu et al. used five modification solutions to modify the surface of RCA to improve its performance. The soybean powder solution had the best modification effect on RCA, with crushing values and WARs of 12.8% and 5.3% at the optimal soaking time of 8 h (Liu et al. 2022). Lin et al. conducted uniaxial compressive tests on 75 specimens with different RCA substitution rates and fiber types to understand the compressive performance of fiber-reinforced RCA. The improvement effect of steel fiber on the energy dissipation capacity and toughness index of recycled concrete was the best, with an average increase of 81.75% and 22.90% (Lin et al. 2023).

Amiri et al. constructed an artificial neural network model to predict the mechanical and durability properties of waste-containing concrete to evaluate the impact of waste on concrete mixes. In addition, the study also used recycled concrete aggregates with replacement levels of 25% and 50%. The results showed that slag could reduce the harmful effects of using recycled concrete aggregates instead of coarse aggregates in the early stages of the sample, and the use of recycled concrete aggregates improved the migration rate of chloride ions in concrete (Amiri and Hatami 2022). Hentges et al. used two treatment methods to explore the best way to improve the performance of recycled concrete aggregates: carbonation and soaking in red brick powder volcanic ash slurry. In the experiment, the treated recycled concrete aggregates were characterized by density, water absorption, mercury intrusion porosity, scanning electron microscopy, petrology, and thermogravimetric analysis. The results showed that the effect of different processing methods on the performance of recycled concrete aggregates varied depending on the target, and appropriate methods needed to be selected according to specific needs (Hentges et al. 2023). To improve the performance of recycled concrete aggregates, experts such as Gholampour used pure graphene suspension (with concentrations of 0, 0.1% and 0.2%) for pre-spraying and pre-soaking treatment and used it as coarse aggregate in concrete. Meanwhile, nano-silica with the same concentration and treatment method was used for comparison. The results showed that graphene was more effective than nanosilica and could significantly improve the strength of concrete, and the concrete performance of pre soaking treatment is better than that of pre spray treatment (Gholampour et al. 2024). Ahmed et al. combined recycled concrete aggregated with drywall waste, scrap tire rubber, and quarry dust to improve their performance in road base applications and reduce construction costs for flexible pavement base. At the same time, the study mixed 0.5% to 2% rubber particles and 5% to 20% drywall waste proportionally into recycled concrete aggregates. The results showed that the CS of the concrete was significantly improved after the addition of these recycled materials (Ahmed et al. 2024).

However, these methods also have certain shortcomings, such as the fact that most studies focus on improving a single performance and lack a comprehensive analysis of the Mechanical And Frost Resistance Properties (MFRP) of recycled concrete. At the same time, some modification methods have high costs or complex processes, which limits their feasibility for practical applications. Therefore, in order to systematically analyze the influence of recycled aggregate with slurry on the mechanical properties and frost resistance of recycled concrete, this study starts with the use of Recycled Aggregate For Grouting (GRA), designs the preparation materials and processes of GRA and recycled concrete. This study aims to improve the performance of recycled concrete and the utilization rate of waste concrete, providing technical support for the resource utilization of construction waste. Its innovation lies in the introduction of GRA to modify concrete, achieving an improvement in the MFRP of concrete. The contribution of this study is the systematic study of the effects of different cement pastes on the basic properties, morphological characteristics, mechanical properties and frost resistance of recycled aggregates and recycled concrete. It provides a theoretical basis and technical support for the efficient utilization of recycled aggregates and the improvement of the performance of recycled concrete, and promotes resource utilization and sustainable development of construction waste.

## Methods and materials

In response to the influence of RCA coating on the MFRP of concrete, this study selects the preparation materials for RCA coating and concrete, and designs the preparation processes for both. In addition, this study designs the methods and indicators for testing the properties of RCA and concrete, and explains the experimental methods for both.

### Selection and preparation of experimental materials

To understand the influence of RCA coating on the performance of concrete, this study first explains the materials required for the experiment, designed the slurry of RCA, and describes the mixing ratio and preparation process of recycled concrete. Second, the testing and experimental methods for the mechanical properties and frost resistance of concrete are explained and designed. Finally, the study validates the mechanical and frost resistance properties of

**Table 1** Number of slurry aggregate

| Group | Used slurry | Age of plasma encapsulation | Group | Used slurry | Age of plasma encapsulation |
|---|---|---|---|---|---|
| A | Nothing | 0 | C3 | 80% PC + 20% silica powder | 15 d |
| B | Portland cement (PC) | 4 d | D | Sulphoaluminate Cement (SC) | 4 d |
| C1 | 80%PC + 20% silica powder | 4 d | E | 70% SC + 30% silicate cement | 4 d |
| C2 | 80%PC + 20% silica powder | 8 d | – | – | – |

RCA and recycled concrete separately to verify the influence of RCA on concrete performance. The experiment uses cement, fly ash, water reducing agent, polymer, water, and aggregate. Among them, cement and fly ash are cementitious materials, and aggregates include fine and coarse aggregates. The cement used in the experiment is ordinary Portland PO42.5 cement and 42.5 grade Sulfoaluminate Cement (SC) from Zidan Construction in Guangzhou, Guangdong. The initial setting time of the two types of cement is 142 min and 18 min, and the final setting time is 187 min and 26 min. The fly ash used is the first grade fly ash from Guangzhou Yueyu Concrete Building Materials, with a moisture content of 30%. In addition, polycarboxylate superplasticizer is used in the experiment, and its dosage is 1% of the cement material. The polymer is silicon powder, with a silicon dioxide content of 92.47%. The water used is all tap water. The fine aggregate is fine sand, and the WAR is 4.8%. The coarse aggregate is RCA, and its concrete strength is C30. The experiment uses a crusher to process coarse aggregates and selects them using a standard of 5–30 mm. The crusher is a PE 150 × 250 jaw crusher. This study uses four types of slurries to modify RCA, namely Portland Cement (PC), 80%PC + 20% silicon powder, SC, and 70%SC + 30% PC. Table 1 shows the numbering of grouting aggregates.

In Table 1, there are a total of seven groups of slurry combinations for grouting aggregates, and the main materials used are PC, silica powder, and SC. In addition, there are three groups of 80%PC + 20% silicon powder coating combinations, corresponding to coating ages of 4 d, 8 d, and 15 d. Finally, there are four types of coating ages for all slurry combinations, namely 0 d, 4 d, 8 d, and 15 d. The preparation process of encapsulated RCA is exhibited in Fig. 1.

In Fig. 1, Step 1 in preparing RCA for slurry coating is to dry mix cement and fly ash mixture for 30 s. Step 2 is to put the dry mixed cementitious material into water and stir for 3 min to form a slurry. Step 3 is to place the slurry into RCA and stir for 3 min. Step 4 is to soak the mixed RCA in a basin until it reaches initial set. Step 5 is to screen using a 5 mm sieve. Step 6 is to air dry for one day and flip it every hour to avoid adhesion of the RCA coating. Step 7 is to harvest and air dry the coated RCA. The calculation of sand consumption $m_s$ per cubic meter of concrete is Eq. (1) (Canhada et al. 2023; Kanta and Ponnada 2022).

$$m_s = V_s \times \rho_s \tag{1}$$

In Eq. (1), $V_s$ and $\rho_s$ are the compacted volume and density of sand per cubic meter of concrete. The water consumption $m_w$ per cubic meter of concrete is solved by Eq. (2).

$$m_w = m_b \times \left(\frac{m_w}{m_b}\right) \tag{2}$$

In Eq. (2), $m_b$ is the mass of cementitious material per cubic meter of concrete. For the analysis of MFRP of

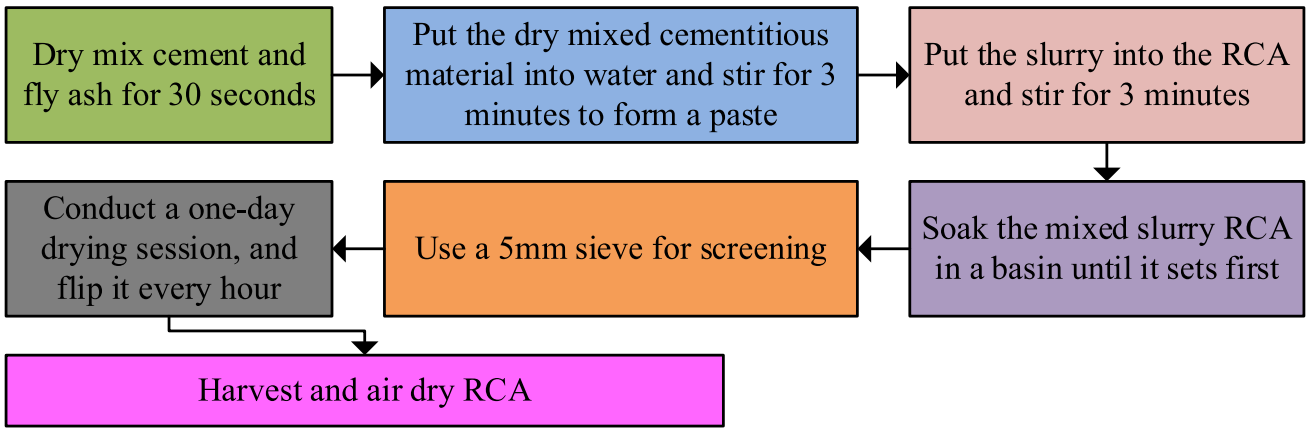



**Fig. 1** Preparation process of recycled aggregate with slurry coating

**Table 2** The mix proportion of concrete

| Group | WCR | Water usage (kg/m$^3$) | Fly ash dosage (kg/m$^3$) | Dosage of cementitious materials (kg/m$^3$) | Sand dosage (kg/m$^3$) | Coarse aggregate dosage (kg/m$^3$) |
|---|---|---|---|---|---|---|
| A-H1 | 0.45 | 202.54 | 247.55 | 450.09 | 627.78 | 1156.36 |
| B-H2 | 0.40 | 190.85 | 286.28 | 477.13 | 620.02 | 1141.94 |
| B-H3 | 0.45 | 202.54 | 247.55 | 450.09 | 627.78 | 1156.36 |
| B-H4 | 0.50 | 212.75 | 212.75 | 425.50 | 634.53 | 1168.89 |
| C1-H5 | 0.45 | 202.54 | 247.55 | 450.09 | 627.78 | 1156.36 |
| C2-H6 | 0.45 | 202.54 | 247.55 | 450.09 | 627.78 | 1156.36 |
| C3-H7 | 0.45 | 202.54 | 247.55 | 450.09 | 627.78 | 1156.36 |
| D-H8 | 0.45 | 202.54 | 247.55 | 450.09 | 627.78 | 1156.36 |
| E-H9 | 0.45 | 202.54 | 247.55 | 450.09 | 627.78 | 1156.36 |

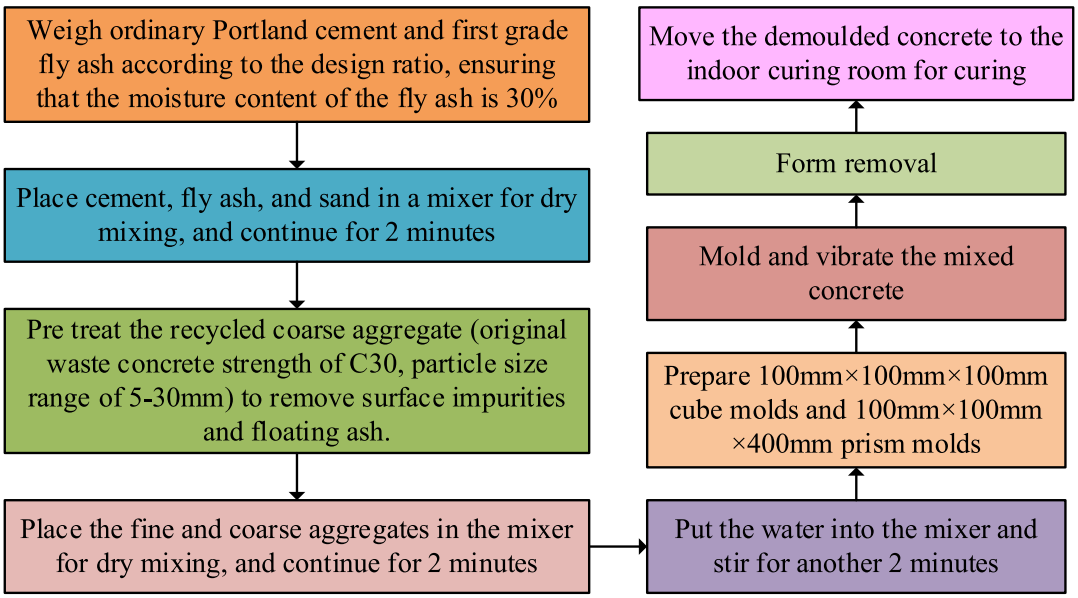



**Fig. 2** The preparation process of recycled concrete

concrete, 100 × 100 × 100 mm concrete cube specimens and 100 × 100 × 400 mm concrete prisms are used in the experiment. Table 2 shows the designed concrete mix proportions.

In Table 2, nine different concrete mix proportions are designed in this study. Among them, there are three values for the Water Cement Ratio (WCR), namely 0.40, 0.45, and 0.50. Similarly, there are three different values for sand dosage, coarse aggregate dosage, dosage of cementitious materials, water usage, and fly ash dosage. In addition, 5.34 kg/m$^3$ of water reducing agent is added to each concrete mix ratio. In addition, three concrete specimens are prepared for each group. The model of the mixer used in the experiment is HJW-30. Figure 2 is the process for preparing recycled concrete.

In Fig. 2, Step 1 in preparing recycled concrete is to weigh ordinary Portland cement and first grade fly ash according to the design ratio, ensuring that the moisture content of the fly ash is 30%. Step 2 is to dry mix cement, fly ash, and sand in sequence in a mixer for 2 min until they are evenly mixed. The step 3 is to pre treat the recycled coarse aggregate (original waste concrete strength C30, particle size 5–30 mm) and remove surface impurities and floating ash. Step 4 is to dry mix the fine and coarse aggregates in the mixer in sequence, and continue for 2 min. Step 5 is to add the water to the blender and blend for another 2 min. Step 6 is to prepare cube molds with dimensions of 100 mm × 100 mm × 100 mm and prism molds with dimensions of 100 mm × 100 mm × 400 mm. Step 7 is to mold and vibrate the mixed concrete, and Step 8 is to remove the mold. Step 9 is to move the demoulded concrete to an indoor curing room for curing, and the temperature in the curing room needs to be maintained at 20 ± 2 °C and the humidity needs to be kept above 95%.

## Design of concrete performance testing and testing methods

To understand the influence of RCA coating on concrete properties, this study tests the concrete properties. Firstly, for the mechanical properties of RCA coated with grout, Particle Size Distribution (PSD), apparent density, crushing index, and WAR are selected as analysis indicators. Secondly, regarding the Mechanical Properties of Recycled Concrete (RCMP), CS, Flexural Strength (FS), and Splitting Tensile Strength (STS) indicators are selected for analysis. Finally, regarding the Frost Resistance of Concrete (CFR), the study selects the Mass Loss Rate (MLR) and Relative Dynamic Modulus (RDM) for analysis. The formula for RCA apparent density $p'$ is Eq. (3) (Zhang et al. 2024; Li et al. 2023b).

$$p' = \left( \frac{M_0}{M_0 + M_2 - M_1} - \beta_t \right) \times 10^3 \tag{3}$$

In Eq. (3), $M_0$ is the constant weight of RCA after drying, and $M_1$ is the total weight of aggregates, water, glass flakes, and wide mouthed bottles. $\beta_t$ is the correction factor. $M_2$ is the total weight of a wide mouthed bottle filled with water and a glass slide. The calculation of WAR is Eq. (4) (Kim and Kim 2021).

$$w = \frac{H_1 - H_2}{H_1} \cdot 100\% \tag{4}$$

In Eq. (4), $H_1$ is the saturated surface dry mass of the aggregate. $H_2$ is the mass of saturated surface dry aggregate after drying. The crushing index is calculated as Eq. (5) (Fang et al. 2020).

$$R = \frac{k_1 - k_2}{k_1} \times 100\% \tag{5}$$

In Eq. (5), $k_1$ is the mass of RCA after drying. $k_2$ is the mass of crushed fine particles. The expression of concrete STS is Eq. (6).

$$F_{ts} = \frac{2T}{\pi A} = 0.637\frac{T}{A} \tag{6}$$

The concrete FS is expressed as Eq. (7) (Najaf et al. 2022).

$$F_{ss} = \frac{TL}{Gh^2} \tag{7}$$

In Eq. (7), $L$ is the span between the supports. $G$ and $h$ are the width and height of the specimen section. The solution of RDM $\varphi_i$ is Eq. (8) (Jajodia and Gadve 2023).

$$\varphi_i = \frac{f_{Ni}^2}{f_{0i}^2} \times 100\% \tag{8}$$

In Eq. (8), $i$ is the $i$-th specimen and $N$ is the number of Freeze–Thaw Cycles (FTC). $f_{0i}$ is the initial transverse fundamental frequency of the concrete specimen. $f_{Ni}$ is the transverse fundamental frequency after the moisture on the surface of the specimen is wiped dry. The calculation of the average RDM $\varphi$ is Eq. (9).

$$\varphi = \frac{1}{3}\sum_{i=1}^{3} \varphi_i \tag{9}$$

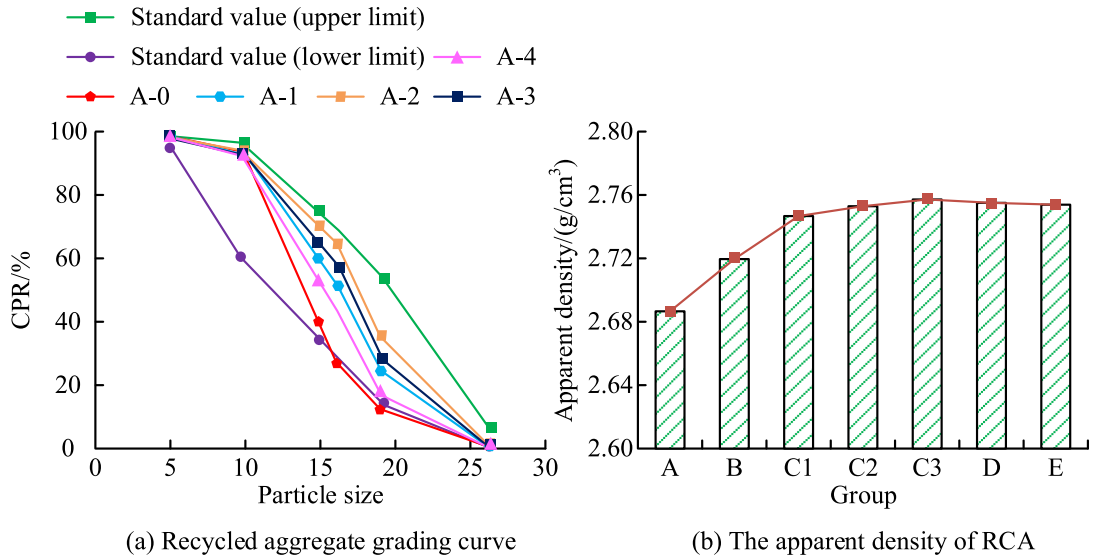
The formula for the MLR $\Delta\theta_{Ni}$ of the specimen is Eq. (10) (Seo et al. 2023).

$$\Delta\theta_{Ni} = \frac{\theta_{0i} - \theta_{Ni}}{\theta_{0i}} \times 100\% \tag{10}$$

In Eq. (10), $\theta_{0i}$ is the initial mass of the test piece. $\theta_{Ni}$ is the mass of the specimen surface after drying off the moisture. The solution for the average MLR $\Delta\theta_N$ of the specimen is Eq. (11).

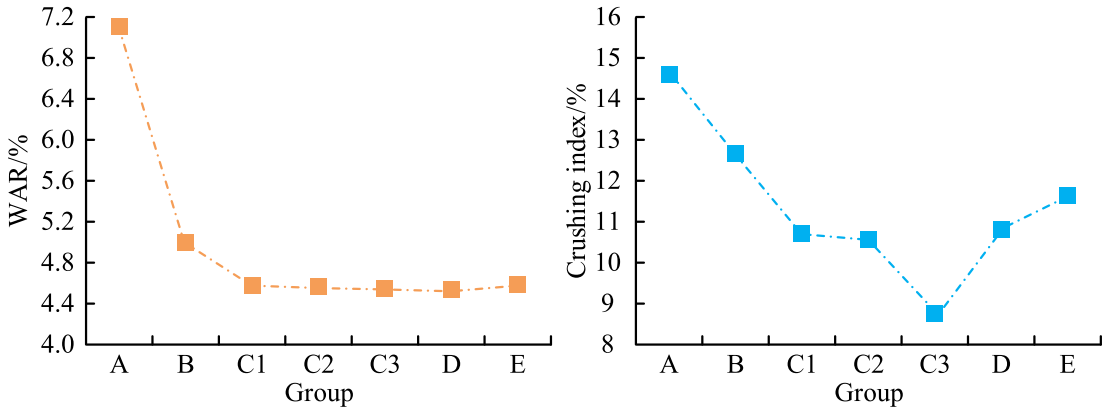
$$\Delta\theta_N = \frac{\sum_{i=1}^{3} \Delta\theta_{Ni}}{3} \times 100\% \tag{11}$$

When testing the RCMP, this study placed it in a hydraulic press with a maximum load of 500 tons. The CS value of mechanical properties needs to be multiplied by a correction factor of 0.95. The correction factor for STS and FS is 0.85. The test of CFR is first completed by the preparation process of concrete, and then the freeze–thaw test is performed. Before conducting the freeze–thaw test, the specimen needs to be cured for one day and demolded. Secondly, the test block needs to be placed in the curing room for 24 days. Afterwards, the test block needs to be soaked for 4 days. Finally, the test block needs to be left in the air for 4 h and the raw data of the test block should be measured. In addition, the number of FTCs is 30, and data is measured once per cycle. To analyze the relationship between the FS and the RCA of the coating, this study conducts another compression and splitting tensile test on the test blocks after the flexural test.




(a) Recycled aggregate grading curve (b) The apparent density of RCA

**Fig. 3** PSD and apparent density results of RCA




(a) WAR of RCA (b) Crushing index of RCA

**Fig. 4** WAR and crushing index results of RCA

## Results

To analyze the influence of encapsulated RCA on the MFRP of concrete, this study first analyzed the performance of encapsulated RCA, including PSD, apparent density, etc. Afterwards, this study analyzed the RCMP from CS, FS, and STS perspectives. Finally, this study analyzed the CFR using MLR and RDM.

### Performance analysis of encapsulated RCA

This study selected 15 RCA samples as a group and processed them using the quartering method. Afterwards, the basic physical properties of the coated RCA are analyzed in an experimental environment at around 20 °C. The PSD and apparent density results of RCA are shown in Fig. 3.

In Fig. 3a, the upper and lower limits of the 15 mm particle size RCA are 74% and 34%, respectively, based on the standard value of Cumulative Percentage Retained (CPR). After encapsulating RCA at ages 0 d, 1 d, 2 d, 3 d, and 4 d, the CPR of RCA with 15 mm particle size is 37.5%, 58.75%, 70%, 64.8%, and 41.9%. After grouting, the particle size of the aggregate has significantly increased, improving the PSD of RCA. In Fig. 3b, after treating RCA with different slurry combinations, the apparent densities of RCA are 2.686 g/cm$^3$, 2.720 g/cm$^3$, 2.748 g/cm$^3$, 2.752 g/cm$^3$, 2.758 g/cm$^3$, 2.756 g/cm$^3$, and 2.754 g/cm$^3$. At the same grouting age and grouting body, the highest apparent density is 2.756 g/cm$^3$ for group D and 2.758 g/cm$^3$ for C3 at 15d. The WAR and crushing index results of RCA are displayed in Fig. 4.

In Fig. 4a, after treating RCA with different slurry combinations, the WAR of RCA is 7.166%, 5.065%, 4.592%, 4.590%, 4.586%, 4.585%, and 4.593%. The maximum

value of WAR appears in group A, and the minimum value appears in group D. In addition, under the same slurry combination, the WAR of C3 is 0.4% less than that of C2, while the WAR of C2 is 0.2% less than that of C1. At the same grouting age, the highest WAR is 5.065% in group B, which is 0.473%, 0.480%, and 0.472% higher than those in groups C1, D, and E. The WAR of the first three groups of samples (A, B, C1) varies greatly. This is because Group A is not grouted, and there are a large number of microcracks and pores on the surface of the aggregate, resulting in a higher WAR. Group B uses ordinary PC slurry, the hydration products of which can fill some pores on the aggregate surface, reduce the water absorption channels, and thus reduce the WAR. The C1 group uses a composite slurry of PC and fumed silica. Silica fume has high pozzolanic activity and can react with cement hydration products to form dense calcium silicate hydrate gel, further filling the pores on the aggregate surface and reducing water absorption. There is no significant change in other samples (C2, C3, D, E), because with increasing grouting age or different slurry compositions, the filling effect gradually approaches saturation or is not as significant as the composite slurry of PC and silica powder, so the change in WAR is not significant.

In Fig. 4b, in terms of crushing index, the maximum value of RCA after grouting treatment is 14.57% of Group A, and the minimum value is 8.86% of C3. The larger the crushing index, the more likely the aggregate is to be damaged. Therefore, the RCA performance after C3 processing is better. The crushing index of the first three groups of samples (A, B, C1) varies widely, which may be due to the large number of microcracks and pores on the surface of the aggregate caused by the lack of grouting in Group A, resulting in a higher crushing index. Group B and Group C1 are treated with ordinary PC slurry and PC silica powder composite slurry, respectively. It can significantly fill the pores on the surface of the aggregate and reduce microcracks, thereby greatly improving the strength of the aggregate and reducing the crushing index. The other samples (C2, C3, D, E) did not show significant changes, because with the extension of the grouting age or changes in the composition of the slurry, their filling and reaction effects have approached their limits or are not as significant as those of the PC-silica powder composite slurry, making the space for further reduction of the crushing index smaller.

## Mechanical performance analysis of concrete under RCA grouting

To analyze the RCMP under RCA grouting, this study analyzes the CS, FS, and STS of recycled concrete. Among them, CS mainly involves the 3D, 7D, and 28D CS of different groups of concrete specimens, and includes the average CS of 3 concrete specimens within each group. Figure 5 shows the CS results of recycled concrete.

In Fig. 5a, on the 3D CS, the average values within each group of recycled concrete in different groups are 32.64 MPa, 38.51 MPa, 33.80 MPa, 27.18 MPa, 32.38 MPa, 34.08 MPa, 30.28 MPa, 37.35 MPa, and 41.87 MPa. This indicates that at the same mix ratio of grout and concrete, the CS is greater when the grout age is 8d. In Fig. 5b, at 7 days of CS, the maximum value of CS is 48.73 MPa for D-H8 and the minimum value is 35.97 MPa for B-H4. The CS of grouted aggregates has been improved to some extent at different ages, and the strength of the aggregates has increased by 27.99%, 8.32%, and 5.55% after treatment for 4 d, 8 d, and 15 d. In addition, the CS of aggregates under C-H5, D-H8, and E-H9 increased by 15.74%, 18.19%, and 16.90% compared to A-H1. In Fig. 5c, at 28 days of CS, the maximum and minimum values of CS are 55.15 MPa for B-H2 and 44.04 MPa for A-H1. The CS of B-H2, B-H3, B-H4, C-H5, C-H6, C-H7, D-H8, and E-H9 increases by 25.23%, 19.16%, 16.55%, 19.98%, 24.59%, 11.42%, 24.02%, and 21.84% respectively compared to A-H1. The reason why the CS of RCA concrete is similar at 3 d, 7 d, and 28 d may be related to the characteristics of the cement hydration process and aggregate properties. Cement hydration occurs rapidly at the early stages (3d and 7d), forming a large amount of hydration products, which significantly improves the early strength of concrete. At 7 days, the hydration process is relatively complete, the concrete structure tends to be stable, and the strength development is close to saturation. Therefore, there is not much difference in intensity between 28 and 7 days. In addition, the grouting treatment improves the interface transition zone between recycled aggregates and cement slurry, which increases the interface strength and further stabilizes the CS of the concrete. While other physical or mechanical properties (e.g., water absorption, splitting tensile strength, etc.) may exhibit significant variation depending on the characteristics or processing methods of the aggregates, these changes do not directly affect the bond strength between the cement slurry and aggregates and the overall rigidity of the concrete. Therefore, the CS of the specimens exhibits a relatively stable characteristic. The improvement of compressive strength is closely related to other properties of concrete. The grouting treatment improves the interface transition zone between the aggregate and cement slurry, enhances the bonding strength between the two, and thus improves the compressive strength. The strengthening of this interface also enhances the performance of concrete when subjected to bending and tensile stresses, resulting in a significant increase in flexural strength and splitting tensile strength. At the same time, the increase in compactness reduces the internal porosity and improves the durability of concrete, such as frost resistance

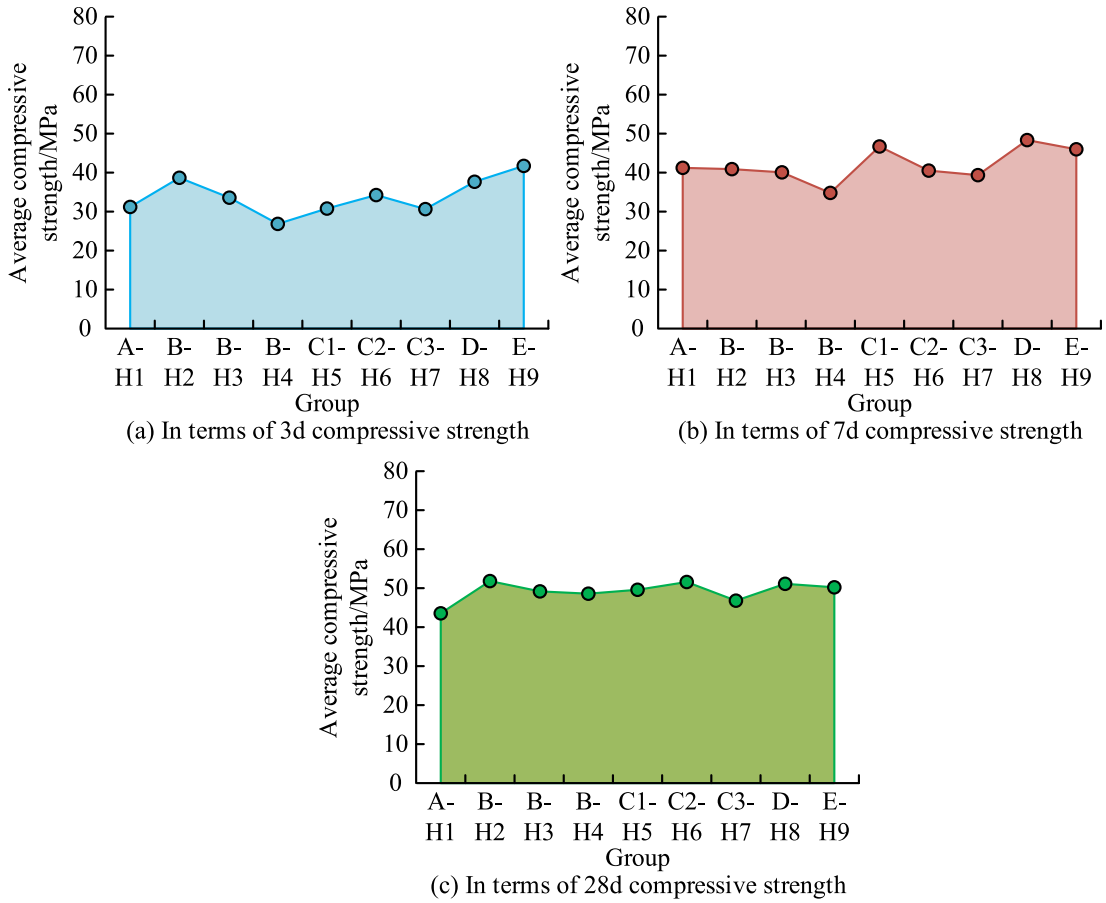



**Fig. 5** Results of CS of recycled concrete

and impermeability. Therefore, the improvement of compressive strength is a manifestation of the optimization of the overall performance of concrete, reflecting the positive impact of interface improvement on mechanical properties and durability. Table 3 shows the FS and STS results of recycled concrete.

In Table 3, compared to A-H1, all groups except B-H4 show improvements of 17.99%, 9.00%, 16.19%, 16.64%, 15.14%, 27.59%, and 25.64% in FS. In B-H2, B-H3, and B-H4, as WCR increases, the FS of recycled concrete gradually decreases. In addition, in C1-H5, C2-H6, and C3-H7, as the grouting age increases, the FS of recycled concrete first increases and then decreases.

On STS, the values of B-H2, B-H3, B-H4, C1-H5, C2-H6, C3-H7, D-H8, and E-H9 are 1.20 MPa, 0.50 MPa, 0.67 MPa, 0.76 MPa, 0.51 MPa, 0.59 MPa, 0.77 MPa, and 1.63 MPa higher than those of A-H1. This indicates that the increase in STS under E-H9 is the largest, at 0.51%. In addition, in B-H2, B-H3, and B-H4, as WCR increases, the STS of recycled concrete first decreases and then increases. Figure 6 shows the Flexural Compression Ratio (FCR) and Tensile Compression Ratio (TCR) of recycled concrete.

Flexural to compressive ratio refers to the ratio of flexural strength to CS of concrete, used to evaluate its toughness and crack resistance. The tensile to compressive ratio refers to the ratio of the tensile splitting strength to the CS of concrete and is used to evaluate the tensile performance of concrete. The higher the FCR and TCR, the better the toughness and crack resistance of concrete, and the FCR of ordinary concrete is between 0.15 and 0.25. In Fig. 6a, the maximum and minimum FCR values are 0.303 and 0.241, corresponding to E-H9 and B-H4. In addition, except for B-H4, the FCR values for all other groups are above 0.25. All other conditions being equal, as WCR increases, FCR decreases. In Fig. 6b, the minimum value of TCR is 0.065 for A-H1, and the maximum value is 0.095 for C2-H6. Compared to A-H1, the TCR of other groups has improved to a certain extent. The comparison between the CS and STS of recycled concrete after folding and ordinary strength is shown in Fig. 7.

According to Fig. 7a, compared with the normal CS after 28 days, all groups show a certain degree of decrease in the folded CS. For example, in the maximum and minimum values of CS, the discounted values are 3.15 MPa and 2.78 MPa smaller than those after 28 days. This is because

**Table 3** Results of FS and STS of recycled concrete

| Group | Flexural/MPa | Group average | STS/MPa | Group average |
|---|---|---|---|---|
| A-H1 | 13.30 | 13.34 | 3.19 | 3.18 |
| | 13.56 | | 3.18 | |
| | 13.17 | | 3.19 | |
| B-H2 | 16.33 | 15.74 | 5.19 | 4.38 |
| | 15.67 | | 4.26 | |
| | 15.23 | | 3.70 | |
| B-H3 | 14.11 | 14.54 | 3.87 | 3.68 |
| | 14.77 | | 3.45 | |
| | 14.74 | | 3.73 | |
| B-H4 | 14.97 | 13.18 | 3.60 | 3.85 |
| | 12.25 | | 4.13 | |
| | 12.32 | | 3.83 | |
| C1-H5 | 16.10 | 15.50 | 3.67 | 3.94 |
| | 15.27 | | 4.00 | |
| | 15.12 | | 4.17 | |
| C2-H6 | 15.69 | 15.56 | 3.87 | 3.69 |
| | 15.56 | | 3.45 | |
| | 15.44 | | 3.73 | |
| C3-H7 | 14.73 | 15.36 | 4.99 | 3.77 |
| | 15.67 | | 2.73 | |
| | 15.69 | | 3.59 | |
| D-H8 | 16.72 | 17.02 | 3.63 | 3.95 |
| | 17.67 | | 4.71 | |
| | 16.68 | | 3.51 | |
| E-H9 | 16.73 | 16.76 | 4.81 | 4.81 |
| | 16.67 | | 5.08 | |
| | 16.88 | | 4.53 | |

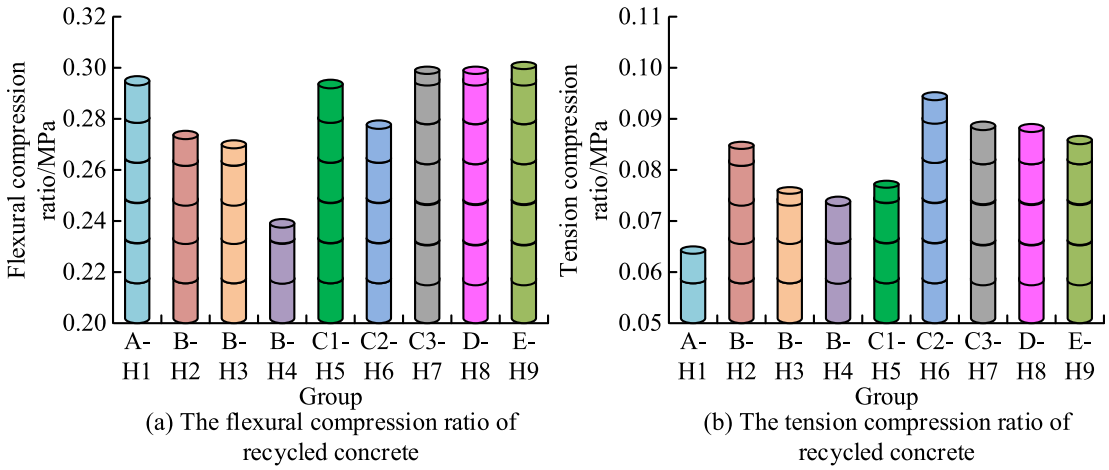
the length and cross-sectional size of the folded compression test block are inconsistent, resulting in an increase in the compression area. In Fig. 7b, the maximum values of splitting CS after 28 days and folding are 4.938 MPa and 4.806 MPa, and the minimum values are 2.778 MPa and 3.186 MPa. In addition, on C2-H6, C3-H7, and D-H8, the post-fracture splitting CS is less than 28 days, while in other groups it is greater than 28 days.

## Analysis of frost resistance of concrete under RCA grouting

To study the effect of RCA coating on the CFR, the MLR and RDM of recycled concrete are analyzed. The experiment sets the termination frequency of FTCs to 360 times, with every 30 cycles being considered as one cycle, and measurement data is required for each cycle. Figure 8 shows the MLR of the specimen under 360 FTCs.

In the comparison of the A-H1, D-H8, and E-H9 groups in Fig. 8a, the MLR of the A-H1 specimen is the highest. As the number of FTCs increases, the MLR of different groups of specimens also increases synchronously. In addition, the maximum MLR values of specimens in groups A-H1, D-H8, and E-H9 are 5.67%, 2.55%, and 2.82%, while the minimum values are 0.26%, 0.07%, and 0.19%. In the comparison of the B-H2, B-H3, and B-H4 groups in Fig. 8b, B-H4 has the highest MLR. All other conditions being equal, as WCR increases, MLR first decreases and then increases. In Fig. 8c, in the comparison of the C1-H5, C2-H6, and C3-H7 groups, the trend of MLR changes decreases first and then increases with the increase of the patina age, and the MLR corresponding to the C2-H6 group is the smallest. In addition, the maximum MLR values for the three groups are 1.85%, 1.43%, and 2.42%, while the minimum values are 0.14%, 0.03%, and 0.04%. Table 4 shows the RDM of the specimens under 360 FTCs.

In Table 4, the maximum RDM values of 9 groups of recycled concrete test blocks are 97.50%, 99.34%, 99.62%, 96.25%, 99.41%, 98.58%, 99.79%, 97.63%, and 97.05%. As the number of FTCs grows, the RDM of the test block gradually decreases. Comparing the test blocks of groups B-H2, B-H3, and B-H4, it can be observed that the larger the WCR, the smaller the RDM of the test block. In addition, the comparison of test blocks in the C1-H5, C2-H6, and C3-H7 groups shows that the older the patina age, the




(a) The flexural compression ratio of recycled concrete

(b) The tension compression ratio of recycled concrete

**Fig. 6** Results of FCR and TCR of recycled concrete

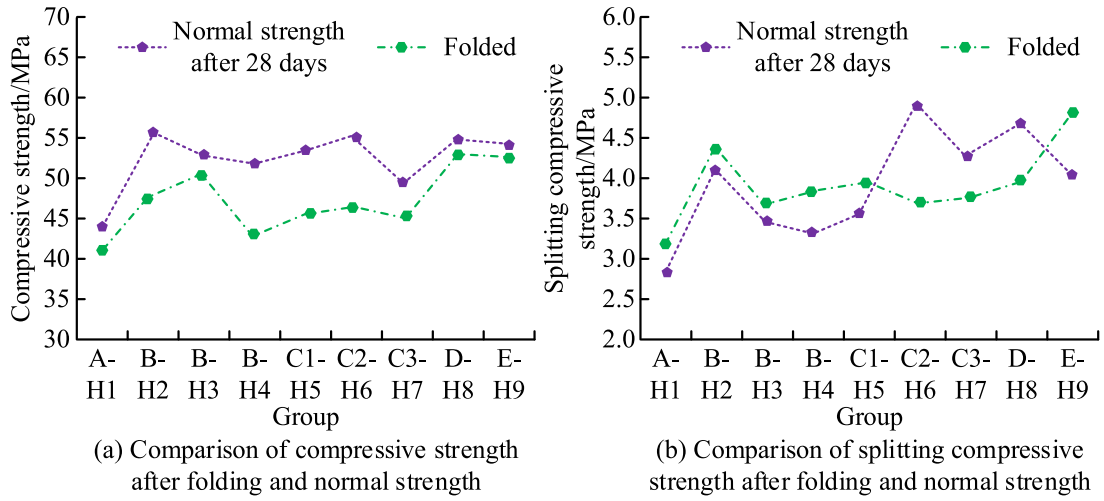



**Fig. 7** Comparison of CS and STS of recycled concrete after bending with ordinary strength

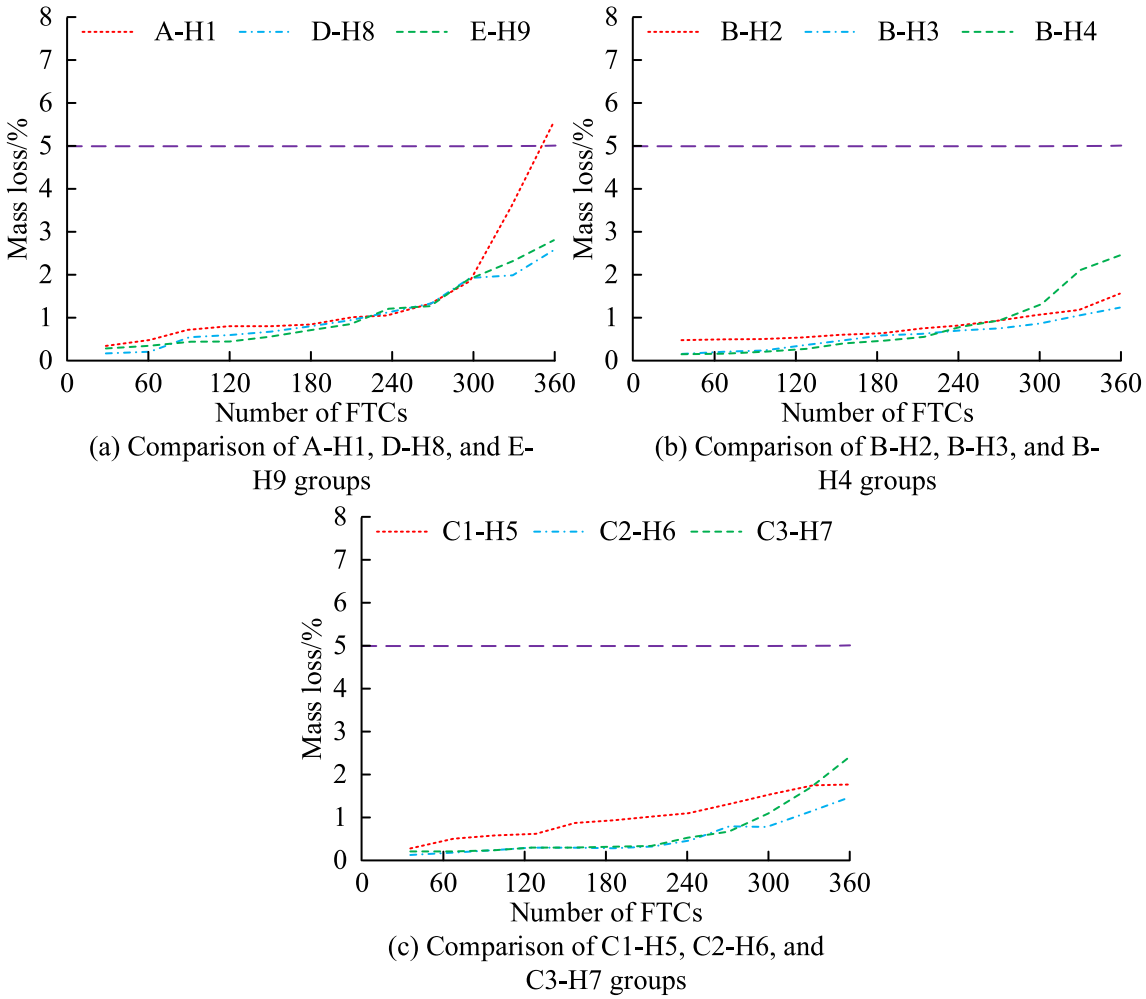



**Fig. 8** Quality loss rate results of specimens under 360 FTCs

**Table 4** Results of RDM of specimens under 360 FTCs/%

| Number of FTCs | Group | | | | | | | | |
|---|---|---|---|---|---|---|---|---|---|
| | A-H1 | B-H2 | B-H3 | B-H4 | C1-H5 | C2-H6 | C3-H7 | D-H8 | E-H9 |
| 30 | 97.50 | 99.34 | 98.87 | 96.25 | 99.41 | 98.58 | 98.88 | 97.63 | 97.05 |
| 60 | 94.36 | 99.22 | 98.87 | 95.42 | 97.34 | 96.50 | 99.21 | 94.74 | 92.39 |
| 90 | 92.88 | 99.28 | 99.32 | 92.03 | 95.26 | 93.72 | 99.41 | 90.93 | 90.96 |
| 120 | 86.73 | 96.86 | 99.62 | 87.41 | 94.09 | 90.43 | 99.79 | 90.93 | 90.96 |
| 150 | 79.40 | 93.13 | 89.79 | 78.48 | 90.71 | 87.10 | 93.52 | 89.04 | 85.58 |
| 180 | 72.72 | 96.15 | 92.16 | 70.01 | 88.56 | 85.63 | 90.24 | 87.05 | 83.05 |
| 210 | 57.99 | 94.39 | 92.52 | 67.65 | 86.21 | 83.60 | 90.27 | 85.62 | 81.81 |
| 240 | 54.85 | 91.81 | 82.69 | 58.92 | 82.66 | 81.71 | 88.63 | 82.80 | 78.27 |
| 270 | 54.20 | 90.81 | 75.13 | 52.91 | 79.29 | 78.21 | 85.21 | 77.90 | 76.70 |
| 300 | 48.53 | 81.69 | 65.04 | 44.74 | 77.81 | 76.20 | 83.05 | 71.90 | 71.30 |
| 330 | 36.95 | 68.07 | 61.21 | 37.96 | 74.42 | 74.70 | 80.41 | 71.90 | 71.30 |
| 360 | – | 58.59 | 49.53 | – | 71.25 | 71.27 | 67.67 | 62.88 | 62.07 |

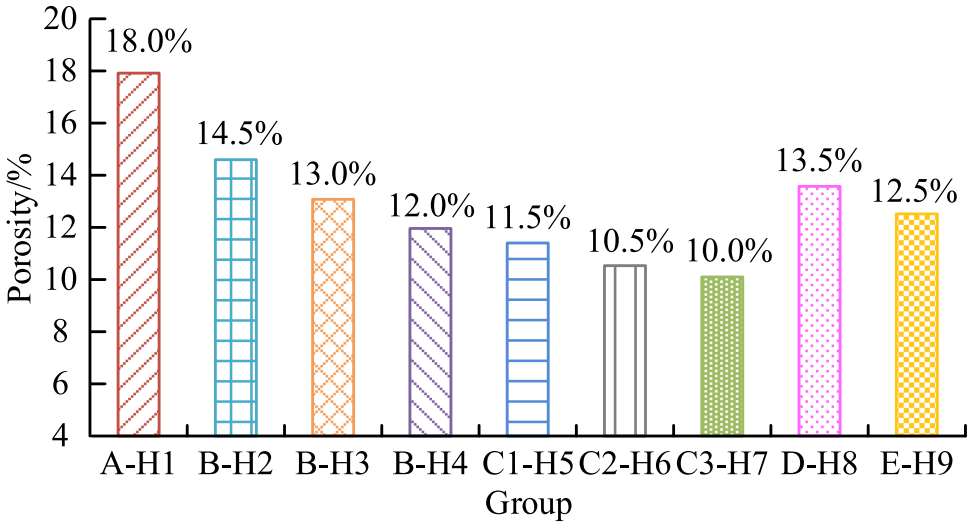



**Fig. 9** Porosity results of interface transition zone in 9 sets of recycled concrete test blocks

smaller the RDM of the test blocks. Overall, RCA coating can effectively improve the CFR. The porosity results of the interface transition zone of 9 sets of recycled concrete test blocks are shown in Fig. 9.

In Fig. 9, the porosity of the interface transition zone of the 9 groups of recycled concrete specimens is 18.0%, 14.5%, 13.0%, 12.0%, 11.5%, 10.5%, 10.0%, 13.5%, and 12.5%, respectively. It can be observed that the interface porosity of the untreated recycled aggregate A-H1 is higher. The porosity of the test blocks (B-H2, B-H3, B-H4) treated with ordinary PC slurry gradually decreases from 14.5 to 12.0% as the grouting age increases. The test blocks (C1-H5, C2-H6, C3-H7) treated with composite slurry of PC and silica powder have a further decrease in porosity from 11.5 to 10.0% due to the filling effect of silica powder. The porosity of the test block treated with sulfoaluminate cement slurry (D-H8) is 13.5%, while the porosity of the test block treated with sulfoaluminate cement and silica cement composite slurry (E-H9) is 12.5%. These data reflect the significant influence of different slurries and processing methods on the porosity of the interfacial transition zone, among which the addition of silica powder and shorter coating age have the most significant effect on reducing porosity.

## Discussion

The study significantly improved the mechanical properties of recycled concrete through grouting treatment, but due to experimental conditions, scanning electron microscopy testing was not conducted to visually demonstrate the changes in microstructure. However, by citing relevant literature, the relationship between microstructure and mechanical properties can be reasonably explained.

Firstly, literature suggests that the microstructure of cement paste, including the formation and distribution of hydration products, as well as the characteristics of capillary pore structure, directly affects the mechanical properties and durability of concrete (Meng et al. 2023). In the study, grouting treatment improved the interface transition

zone between aggregates and cement slurry by filling micro cracks and pores on the surface of aggregates, thereby enhancing the compactness and strength of concrete. The optimization of this microstructure reduces the internal porosity, enhances the interfacial bonding strength, and thereby improves the compressive strength and splitting tensile strength of concrete.

Secondly, there is also literature indicating that the morphology and distribution of aggregates have a significant impact on the mechanical properties of concrete. The surface of the aggregate after grouting treatment is smoother and the particle shape is more regular, which helps to reduce stress concentration inside the concrete and improve its overall performance (Hu et al. 2024). In addition, the use of additives can also affect the microstructure and properties of concrete (Su et al. 2023). In the study, the microstructure of concrete was further optimized and its mechanical properties were improved by adding additives such as silica powder to the slurry.

In summary, although this study did not directly conduct SEM testing, the relationship between microstructure and mechanical properties can be reasonably explained by citing relevant literature. Future research can consider using advanced testing methods such as SEM to more intuitively observe and analyze changes in microstructure, thereby further verifying and deepening the conclusions of this study.

## Conclusion

To analyze the influence of RCA coating on MFRP of concrete, this study designed the materials and preparation processes required for coating aggregates and recycled concrete, and constructed the mix proportions of the two. The results indicated a significant increase in the particle size of the aggregate after grouting. Under different slurry combinations, the apparent density of RCA was 2.686 g/cm$^3$, 2.720 g/cm$^3$, 2.748 g/cm$^3$, 2.752 g/cm$^3$, 2.758 g/cm$^3$, 2.756 g/cm$^3$, and 2.754 g/cm$^3$. At the same grouting age, the highest WAR was 5.065% in Group B. The maximum and minimum crushing indices of RCA coated with grout were 14.57% and 8.86%, respectively. It can be concluded that grouting technology could effectively improve the basic properties of recycled aggregates. Under 7 days of CS, the CS of aggregates under C-H5, D-H8, and E-H9 increased by 15.74%, 18.19%, and 16.90% compared to the CS of A-H1. On FS, compared to A-H1, except for B-H4, all other groups have improved by 17.99%, 9.00%, 16.19%, 16.64%, 15.14%, 27.59%, and 25.64%. In addition, the increase in STS under E-H9 was the largest, with a value of 0.51%. Except for B-H4, the FCR values for all other groups were above 0.25. The maximum and minimum values of TCR were 0.095 and 0.065. Compared with the normal CS after 28 days, all groups showed a certain degree of decrease in post folding CS. After 28 days, the maximum values of folded CS and split CS were 4.938 MPa and 4.806 MPa. The maximum and minimum MLR values of recycled concrete specimens were 5.67% and 0.03%, while the maximum and minimum RDM values were 99.79% and 36.95%. In summary, the recycled concrete treated with grout shows significant improvements in CS, flexural strength, splitting tensile strength, and freeze resistance, among which the recycled concrete treated with PC silica powder slurry performs best in all performance aspects. The limitation of this study is that it only analyzed the 2D indicators of recycled aggregates, which can only reflect the characteristics of a certain aspect of the aggregates. Future research can utilize other methods to analyze the 3D characteristics of aggregates.

**Author contributions** Xuan Wang provided the concept and wrote the draft, and Mengting Fan revised this paper critically. Both authors reviewed this paper carefully and approved this submission.

**Funding** The research is supported by the Science and Technology Research Program of Chongqing Municipal Education Commission (No. KJQN202101302).

**Data availability** All data generated or analyzed during this study are included in this article. Further enquiries can be directed to the corresponding author.

## Declarations

**Conflict of interest** The author declares that there's no conflict of interest.

**Ethics approval** An ethics statement was not required for this study type, no human or animal subjects or materials were used.

**Consent to participate** Not applicable.

**Consent for publication** Not applicable.

## References

Ahmed, A., Shah, S.K.H., Ahmad, N., Ali, U., Malik, A.A., Iqbal, M.J.: Feasibility of utilizing recycled concrete aggregate blended with waste tire rubber and drywall waste as pavement subbase material. J. Mater. Cycles Waste Manag. **26**(4), 2278–2293 (2024)

Amiri, M., Hatami, F.: Prediction of mechanical and durability characteristics of concrete including slag and recycled aggregate concrete with artificial neural networks (ANNs). Constr. Build. Mater. **325**, 126839 (2022)

Canhada, J.C.S., Paiva, F.F.G., Shinohara, G.M.M., Okimoto, F., Hiranobe, C.T., Teixeira, S.R.: Production of new concrete with leather tannery waste used as partial replacement of the natural sand. J. Mater. Cycles Waste Manag. **25**(2), 944–953 (2023)

Chen, Z., Feng, Q., Yue, R., Chen, Z., Moselhi, O., Soliman, A.: Construction, renovation, and demolition waste in landfill: a review

of waste characteristics, environmental impacts, and mitigation measures. Environ. Sci. Pollut. Res. **29**(31), 46509–46526 (2022)
Fang, H.Y., Liu, F.L., Yang, J.H.: Highquality coarse aggregate recycling from waste concrete by impact crushing. J. Mater. Cycles Waste Manag. **22**(3), 887–896 (2020)
Gharibi, H., Mostofinejad, D.: Thermal and mechanical properties of concrete containing porcelain ceramic tile waste as fine and coarse aggregates. Mag. Concr. Res. **75**(3), 123–134 (2023)
Gholampour, A., Sofi, M., Tang, Y.: Effect of treatment method of recycled concrete aggregate by pristine graphene on mechanical and durability properties of concrete. Mag. Concr. Res. **76**(14), 769–782 (2024)
He, Z., Shen, A., Wang, X., Wu, J., Wang, L.: Effect of modification treatment on chloride ions permeability and microstructure of recycled brick-mixed aggregate concrete. J. Wuhan Univ. Technol. Mater. Sci. Ed. **39**(3), 728–737 (2024)
Hentges, T.I., Kautzmann, V.O., Angulo, S.C., de Souza Kazmierczak, C., Mancio, M., Sander, A., Kulakowski, M.P.: Comparative study of porous recycled concrete aggregates treated with pozzolanic slurry or carbonation and resulting recycled concrete properties. Int. J. Civ. Eng. **21**(12), 1965–1984 (2023)
Hu, J., Sheng, D., Qin, F., Huo, X., Chai, Z.: Mechanical properties of hybrid fiber-reinforced recycled coarse aggregate concrete based on DIC method. Bull. Chin. Ceram. Soc. **43**(10), 3745–3754 (2024)
Jajodia, R., Gadve, S.: Development of statistical model for prediction of modulus of elasticity of concrete. Struct. Concr. **24**(3), 4297–4312 (2023)
Kanta, N.R., Ponnada, M.R.: Performance of spent garnet sand and used foundry sand as fine aggregate in concrete. World J. Eng. **19**(5), 632–638 (2022)
Kim, N.W., Kim, M.H.: Proper mix proportion and construction method of waste concrete using recycled coarse aggregate in site considering environment. J. Civ. Constr. Environ. Eng **6**(6), 202–207 (2021)
Li, J., Chen, L.L., Wang, W.Y.Q.: Effect of modification and replacement rate of recycled coarse aggregate on properties of recycled aggregate concrete. Iran. J. Sci. Technol. Trans. Civ. Eng. **47**(6), 3321–3332 (2023a)
Li, J., Chen, L.L., Wang, W.Y.Q.: Effect of modification and replacement rate of recycled coarse aggregate on properties of recycled aggregate concrete. Iran. J. Sci. Technol. Trans. Civ. Eng **47**(6), 3321–3332 (2023b)
Li, Z., Bian, Y., Zhao, J., Wang, Y., Qiu, X., Liu, Q.: Sustainable building materials-recycled aggregate and concrete: a systematic review of properties, modification techniques, and environmental impacts. Environ. Sci. Pollut. Res. **31**(14), 20814–20852 (2024)
Lin, G., Liu, K., Chen, Y., Ji, Y., Jiang, R.: Experimental investigation on compressive properties of fiber recycled aggregate concrete. J. Renew. Mater. **11**(11), 3957–3975 (2023)
Liu, X., Liu, L., Zuo, J., Zhao, P., Xie, X., Li, S.: Evaluation of various modification methods for enhancing the performance of recycled concrete aggregate. J. Renew. Mater. **10**(10), 2685–2698 (2022)
Meng, S., Li, X., Liu, Z., Guan, M.: Bond-slip constitutive model of recycled coarse aggregate concrete with limestone manufactured sand in square steel tubes. J. Archit. Civ. Eng. **40**(1), 38–48 (2023)
Najaf, E., Abbasi, H., Zahrai, S.M.: Effect of waste glass powder, microsilica and polypropylene fibers on ductility, flexural and impact strengths of lightweight concrete. Int. J. Struct. Integr. **13**(3), 511–533 (2022)
Seo, W., Choi, B., Shin, D.K.J.: Development of a quality management system for precast concrete factories. J. Civ. Eng. Manag. **29**(5), 475–486 (2023)
Su, W., Chen, Z., Liao, H., Liu, D., Zhou, X.: Mechanical properties of steel-polypropylene fiber reinforced fully recycled coarse aggregate concrete. Adv. Concr. Constr. **16**(3), 127–139 (2023)
Supsup, H.V., Galavote, T., Brumatti, D., Diniz Chaves, G.D.L., Siman, R.R.: An economic assessment model of construction and demolition waste management based on system dynamics: a case study in the city of serra-es. Environ. Eng. Manag. J. **22**(5), 859–870 (2023)
Yousheng, D., Keqin, Z., Zhigang, H.Y.: Analysis and optimization of design parameters for recycled concrete modified with nano? CaCO_3 considering environmental and economic and mechanical properties. J. Mater. Cycles Waste Manag. **25**(6), 3651–3663 (2023)
Zhang, M., Yang, X., Ding, Y., Sun, B., Zhang, X., Lü, X.: High-efficiency carbonation modification methods of recycled coarse aggregates. J. Wuhan Univ. Technol. Mater. Sci. Ed. **39**(2), 386–398 (2024)

**Publisher's Note** Springer Nature remains neutral with regard to jurisdictional claims in published maps and institutional affiliations.

Springer Nature or its licensor (e.g. a society or other partner) holds exclusive rights to this article under a publishing agreement with the author(s) or other rightsholder(s); author self-archiving of the accepted manuscript version of this article is solely governed by the terms of such publishing agreement and applicable law.